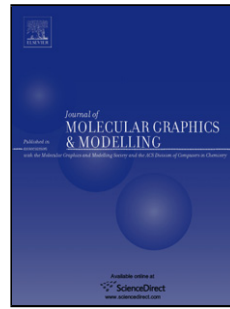


Accepted Manuscript

Title: Molecular docking and molecular dynamics simulation studies of *Trypanosoma cruzi* triosephosphate isomerase inhibitors. Insights into the inhibition mechanism and selectivity



Author: Lucía Minini Guzmán Álvarez Mercedes González
Hugo Cerecetto Alicia Merlino

PII: S1093-3263(15)00036-4

DOI: <http://dx.doi.org/doi:10.1016/j.jmgm.2015.02.002>

Reference: JMG 6518

To appear in: *Journal of Molecular Graphics and Modelling*

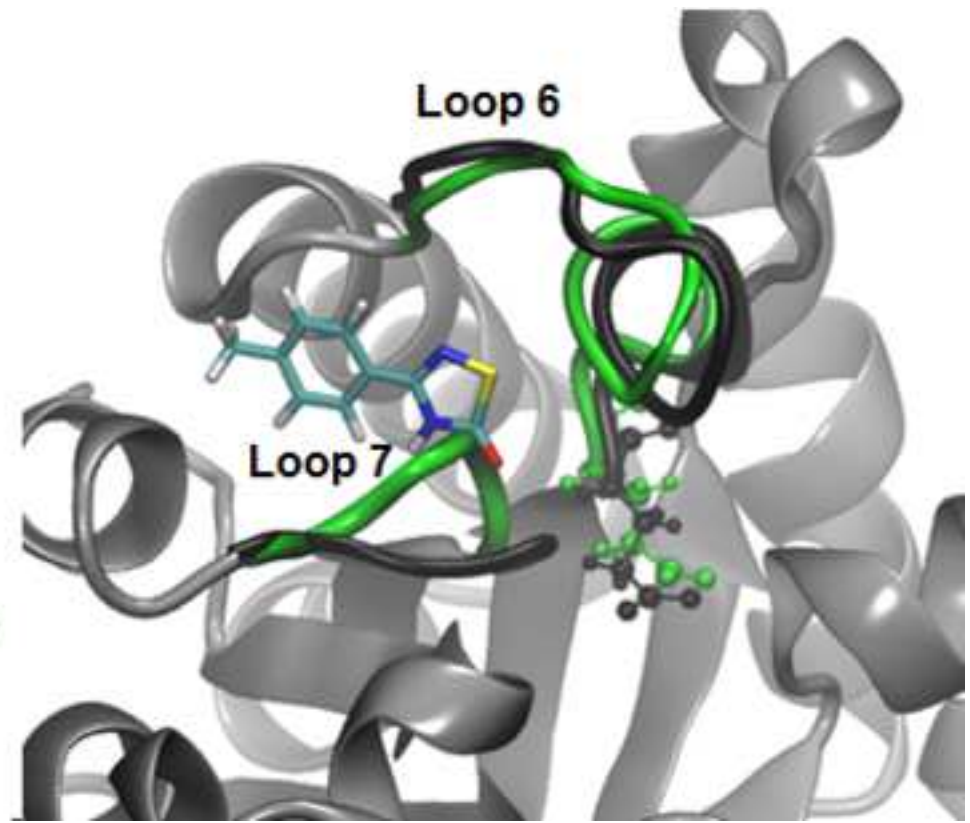
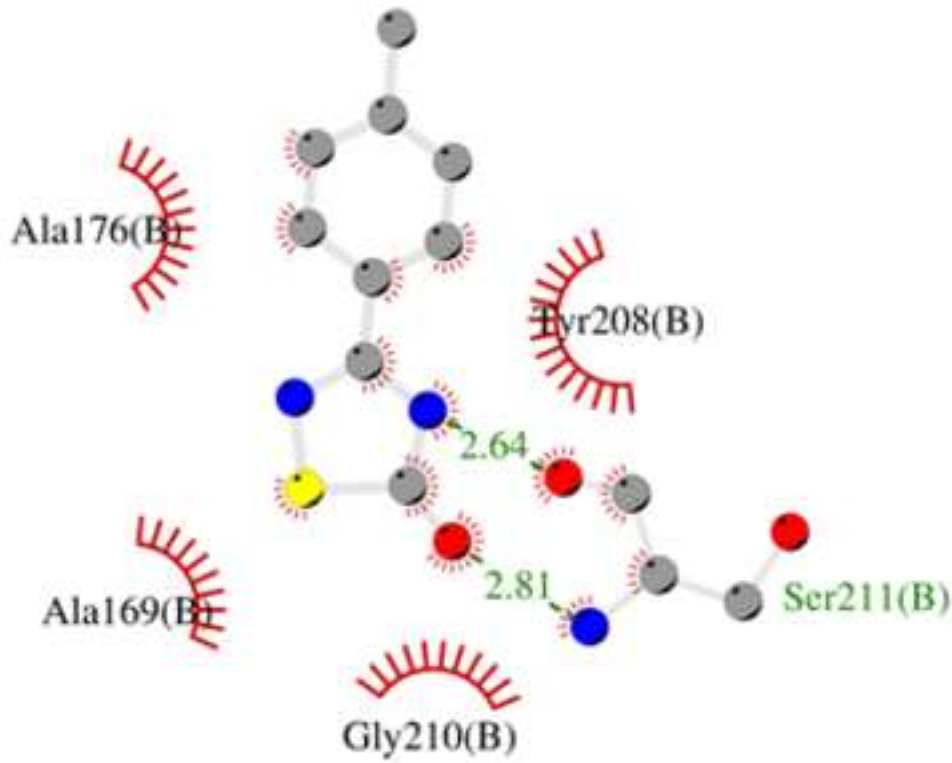
Received date: 25-5-2014

Revised date: 22-11-2014

Accepted date: 12-2-2015

Please cite this article as: L. Minini, G. Álvarez, M. González, H. Cerecetto, A. Merlino, Molecular docking and molecular dynamics simulation studies of *Trypanosoma cruzi* triosephosphate isomerase inhibitors. Insights into the inhibition mechanism and selectivity, *Journal of Molecular Graphics and Modelling* (2015), <http://dx.doi.org/10.1016/j.jmgm.2015.02.002>

This is a PDF file of an unedited manuscript that has been accepted for publication. As a service to our customers we are providing this early version of the manuscript. The manuscript will undergo copyediting, typesetting, and review of the resulting proof before it is published in its final form. Please note that during the production process errors may be discovered which could affect the content, and all legal disclaimers that apply to the journal pertain.



Highlights

- MD simulations of apo-TcTIM and hTIM in solution are performed
- The binding mode and mechanism of action of three TcTIM inhibitors are proposed
- We found interfacial hot spots that should be considered in novel drug design
- The selectivity of these inhibitors against TcTIM are explained based on MD results

Molecular docking and molecular dynamics simulation studies of *Trypanosoma cruzi* triosephosphate isomerase inhibitors. Insights into the inhibition mechanism and selectivity

Lucía Minini^{a,b}, Guzmán Álvarez^b, Mercedes González^b, Hugo Cerecetto^{b,c}, Alicia Merlino^{a*}

^a Laboratorio de Química Teórica y Computacional, Instituto de Química Biológica, Facultad de Ciencias, Universidad de la República, Montevideo, Uruguay. ^b Grupo de Química Medicinal, Laboratorio de Química Orgánica, Facultad de Ciencias, Universidad de la República, Montevideo, Uruguay. ^c Área de Radiofarmacia, Centro de Investigaciones Nucleares, Facultad de Ciencias, Universidad de la República, Montevideo, Uruguay

Abstract

Trypanosoma cruzi (*T. cruzi*) triosephosphate isomerase (TcTIM) is a glycolytic enzyme essential for parasite survival and has been considered an interesting target for the development of new antichagasic compounds. The homodimeric enzyme is catalytically active only as a dimer. Interestingly, significant differences exist between the human and parasite TIMs interfaces with a sequence identity of 52%. Therefore, compounds able to specifically disrupt TcTIM but not Homo sapiens TIM (hTIM) dimer interface could become selective antichagasic drugs. In the present work, the binding modes of 1,2,4-thiadiazol, phenazine and 1,2,6-thiadiazine derivatives to TcTIM was investigated using molecular docking combined with molecular dynamics (MD) simulations. The results show that phenazine and 1,2,6-thiadiazine derivatives, 2 and 3, act as dimer-disrupting inhibitors of TcTIM having also allosteric effects in the conformation of the active site. On the other hand, the 1,2,4-thiadiazol derivative 1 binds into the active site causing a significant

decrease in enzyme mobility in both monomers. The loss of conformational flexibility upon compound 1 binding suggests that this inhibitor could be preventing essential motions of the enzyme required for optimal activity. The lack of inhibitory activity of 1 against hTIM was also investigated and seems to be related with the high mobility of hTIM which would hinder the formation of a stable ligand-enzyme complex. This work has contributed to understand the mechanism of action of this kind of inhibitors and could result of great help for future rational novel drug design.

Keywords: TcTIM; hTIM; TcTIM-inhibitors; molecular docking; molecular dynamics; selective TcTIM inhibitors; dimer-disrupting inhibitors; rational drug design.

Abbreviations¹

*Corresponding author: Prof. Alicia Merlino. Phone: +598-25252186; Fax: +598-25250749, e-mail: amerlino@fcien.edu.uy. Postal Adress: Laboratorio de Química Teórica y Computacional, Instituto de Química Biológica, Facultad de Ciencias, Universidad de la República, Iguá 4225, Montevideo, 1140, Uruguay.

1. Introduction

Trypanosoma cruzi (*T. cruzi*), the causative agent of Chagas' disease, is a unicellular eukaryotic protozoa which causes about 12,500 deaths per year [1]. This disease mainly affects the poorest

¹ TcTIM: Trypanosoma cruzi triosephosphate isomerase; hTIM: Homo sapiens triosephosphate isomerase; MD: molecular dynamics; SD: steepest descent; CG: conjugate gradient; SASA: solvent accessible surface area.

communities in Latin America, which do not represent a profitable market for pharmaceutical companies [2]. The economic burden of Chagas' disease is similar to those of other prominent diseases, even in non-endemic countries, suggesting an urgent need for efforts toward control of the disease [3]. Pharmacotherapy against *T. cruzi* involves the use of two drugs, Nifurtimox and Benznidazole. However, certain apprehension exists regarding the application of these compounds because of the side effects in the host, its variable efficacy and the emergence of resistant strains [4]. Moreover, the antigenic variation expressed by the parasite in different stages of its life cycle has hampered progress in vaccine development [5]. It is clear that new approaches are needed in order to produce highly specific antichagasic drugs, and thus, the development of drugs targeted against key parasitic enzymes is currently a field of intense research [6-8]. Enzymes of the glycolytic pathway are potential targets, since trypanosomes rely mainly on glycolysis as an energy source [9]. Therefore, blocking this pathway could result in an energy deficit that might impair the survival of the parasite. In fact, triosephosphate isomerase (TIM) has been considered as a potential target for drug design in several parasites [10-13]. TIM is a homodimeric enzyme that catalyzes the reversible isomerization of glyceraldehyde-3-phosphate and dihydroxyacetone phosphate, an important step in the glycolytic pathway [14]. While *Homo sapiens* TIM (hTIM) and *T. cruzi* TIM (TcTIM) have the same catalytic residues, there are regions of highly divergent amino acid sequences that have been exploited in order to attain selective inhibition [15-18]. According to biochemical assays, most of the identified selective compounds seem to alter the enzymatic activity by perturbing the dimer interface. However, in most cases the exact binding mode is unknown due to the lack of crystallographic structures of ligand-enzyme complexes. In the last years many attempts have been made to predict the binding modes of selective inhibitors through molecular docking calculations [19-24]. Although protein-ligand docking is largely used as a first approach in the identification of new lead compounds for drug design, the success of this

technique depends heavily on the characteristics of the protein. Docking algorithms, as implemented in current docking programs, deal with flexible ligand while receptor flexibility is not taken into account or is treated in a very crude manner considering just local rearrangements [25]. Allowing for protein flexibility is fundamental when large-scale conformational changes play a key role both in catalysis and ligand recognition and binding, as occurs in TIM [26]. In this sense, the combination of docking calculations and molecular dynamics (MD) simulations have been successfully used in rational drug design to improve initial docking results [27-29] and to get molecular-level understanding of inhibition mechanisms [30]. Moreover, MD can be used during the preparation of the protein receptor before docking to obtain alternative conformations that can be combined into an average structure to account for conformational changes that may be critical for the binding process [27].

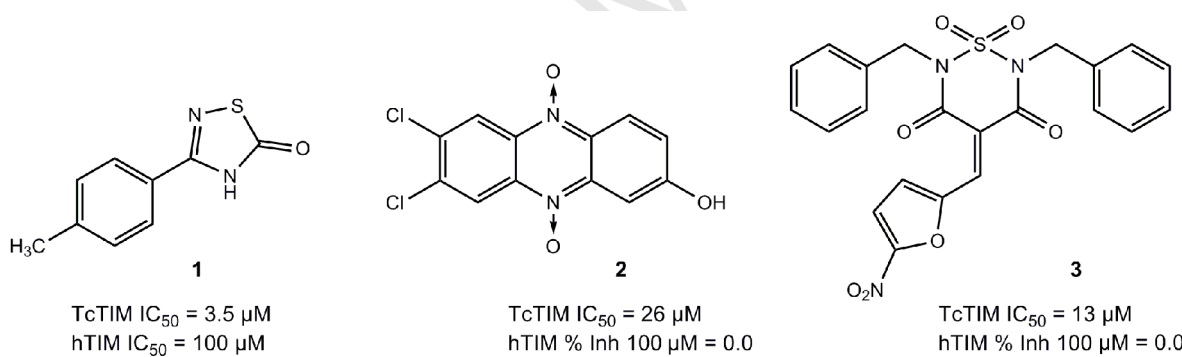


Fig. 1. Chemical structures and inhibitory activity of compounds used in this study.

In the last years we have been working in the development of selective compounds against TcTIM [15,19,30]. Thus, a set of new inhibitory chemotypes like 1,2,4-thiadiazole, phenazine and 1,2,6-thiadiazine have emerged with appropriate selectivity profiles. Three of these novel compounds (Fig. 1) act as selective and non-competitive inhibitors of TcTIM. Previous molecular docking studies were performed with these derivatives [19] but the flexibility of the enzyme before and after ligand binding was not taken into account. Therefore, the detailed binding mode and the

mechanisms responsible for the inhibitory effect are still unexplored. In the present study, a multistep framework by combining molecular docking and MD simulations was applied in order to explore the binding modes of these inhibitors into TcTIM and to study the conformational changes induced in the enzyme by bound ligands. These results have contributed to understanding the mechanism of inhibition of these novel compounds, a necessary step to obtain more selective and potent drugs for this target. After that, we selected the best inhibitor of TcTIM, compound 1, and modeled the ligand-hTIM complex to determine the factors that account for the compound selectivity.

2. Materials and methods

2.1. Preparation of protein structures

The X-ray structures of unliganded TcTIM and hTIM were retrieved from the Protein Data Bank (<http://www.rcsb.org/pdb>); accession codes 1TCD and 2JK2, respectively. MD calculations were performed using the sander module implemented in the Amber 12 suite [31], with the ff03.r1 force field [32]. Hydrogen atoms and chloride ions (to neutralize charge) were added to each protein with the leap utility. Each system was placed in a truncated octahedral box of TIP3P explicit water [33], extended 10 Å outside the protein on all sides. The structures of TcTIM and hTIM were treated as follows: a) water and counterions were relaxed to minimize energy during 2,000 steps (500 steepest descent steps, SD, and 1,500 conjugate-gradient steps, CG) with the protein restrained with a force constant of 500 kcal/molÅ²; b) the system was minimized without restraints during 15,000 steps (5,000 SD and 10,000 CG). Long range interactions were considered using the particle-mesh Ewald (PME) method [34] and a non-bonded interactions cutoff of 10 Å

was used. After minimization, each system was gradually heated in a NVT ensemble from 0 to 300 K over 100 ps using the Berendsen coupling algorithm [35]. This procedure was followed by 5 ns of NPT simulations at 300 K and 1 atm pressure using the Langevin dynamics algorithm [36]. All bonds involving hydrogen atoms were constrained using the SHAKE algorithm [37]. A time step of 2.0 fs was used for all production dynamics and coordinates of the systems were saved every 0.2 ps. The average structures of TcTIM and hTIM over the last 4 ns of the trajectories were computed with the ptraj package in AmberTools 12 and used for subsequent docking calculations.

2.2. Preparation of inhibitor structures

Compounds 1-3 (Fig. 1) were fully optimized at the B3LYP/6-31G(d,p) [38,39] level in water using the IEF-PCM continuum model [40] with Bondi atomic radii. The nature of the optimized structures as stable species was inspected checking the eigenvalues of the analytic Hessian matrix, calculated at the same level of theory, to be positive in all the cases. All these calculations were performed using the Gaussian09 software [41].

2.3. Ligand-protein molecular docking

To predict the binding site of compounds 1-3 into TcTIM and of compound 1 into hTIM, flexible-ligand docking was performed using a grid box of 124×126×126 points with a grid spacing of 0.603 Å in order to cover the entire protein surface (blind docking). The grid box was centered on the macromolecule. Once the binding site was determined, the free energies of binding were refined using a smaller grid box sized 60x60x66 points with a spacing of 0.375 Å, now centered at the ligand binding site. Results differing by less than 2.0 Å in root-square deviation were grouped in

the same cluster. The conformation with the lowest binding energy was chosen from the most populated cluster and the corresponding ligand-protein complex was used for further MD studies.

All docking calculations were done with the AutoDock 4.2 [42] software package using the Lamarckian genetic algorithm. A population size of 150 individuals and 2.5×10^6 energy evaluations were used for 50 search runs. For the rest of the parameters default values were employed.

2.4. Ligand-protein molecular dynamics

Ligand-TIM MD was performed as described in Section 2.1 using the GAFF [43] force field for ligands. RESP partial charges for compounds 1-3 were derived using Gaussian09 [41] at the HF/6-31G* level and the antechamber module was employed to obtain the force field parameters.

2.5. Trajectory analysis

The stability of unbounded TIMs and the corresponding inhibitor-enzyme complexes was checked from the root mean square deviation (RMSD) and the flexibility of the systems was evaluated from the root mean square fluctuations (RMSF). For RMSD calculations energy-minimized structures were used as the reference structure. RMSFs were calculated relative to the averaged structures. RMSD and RMSF analyses were performed using the ptraj utility. Solvent accessible surface area (SASA) over selected interfacial residues for apo-TcTIM and TcTIM-inhibitor complexes was calculated using cpptraj.

3. Results and discussion

3.1. Molecular dynamics of unliganded TcTIM and hTIM

It has been reported that TIM's conformational changes and dynamic behavior are fundamental for both catalytic activity and ligand binding [44]. Optimal function of TIM relies on the ability of an active site loop (loop 6, residues 166 to 177) to move between open and close conformations [45], being the open conformation the preferred state in apo-TIM [46]. In general, all the dimeric TIM crystal structures have one chain open and the other chain closed due to crystal packing effects and this fact could significantly affect proper docking prediction of ligand binding modes. Taking into account the importance of protein conformation in the final outcome of a docking assessment, 5 ns of MD simulations of apo-enzymes in solution were performed to obtain representative structures with an adequate disposition to accommodate the ligand for further docking studies. TcTIM and hTIM C α RMSD values (compared to the energy minimized starting structure) along the simulations are shown in Fig. 2. As seen, following a 0.5 ns rapid increase the RMSD of both enzymes remains stable along the entire simulation time indicating that the system reached equilibrium. From 0.5 ns to the end, the C α RMSD average values for TcTIM and hTIM are 1.20 \pm 0.09 Å and 1.08 \pm 0.09 Å, respectively.

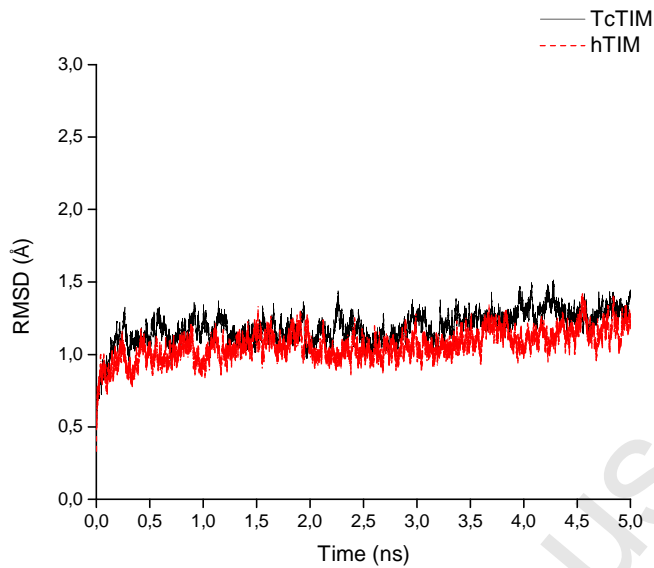


Fig. 2. Comparison of C_α RMSD (relative to the energy minimized starting structure) as a function of time for TcTIM (solid black line) and hTIM (dashed red line) along 5 ns MD simulations.

Examination of monomers A and B RMSF profiles for TcTIM and hTIM reveals that significant mobility differences are present between both chains (Fig. 3). However, the pattern of more mobile residues is equal in both monomers and coincides with loop regions. In particular, the higher peak corresponds to residues of the catalytic loop 6 (residues 166 to 177) and an adjacent α -helix (residues 120 to 140) that moves along with this loop. RMSF analysis points out that flexibility differences between the two subunits are also observed in solution and therefore are not only a consequence of each subunit crystal packing as previously reported [47].

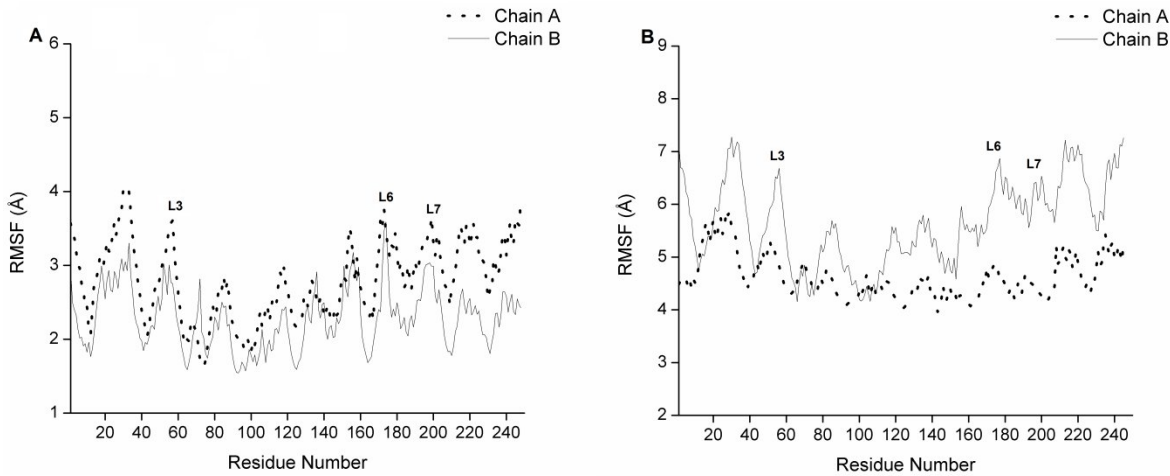


Fig. 3. C^α RMSF of monomers A and B for TcTIM (A) and hTIM (B). L3, L6 and L7 refer to loop 3, loop 6 and loop 7, respectively.

As can be seen in Fig. 3 there is a notorious difference in the dynamic behavior of TcTIM and hTIM. This is an interesting finding since the selectivity shown by most inhibitors against TcTIM could be related to the ability of this enzyme to form more stable enzyme-inhibitor complexes due to its lower mobility.

Superimposition of the average structures of TcTIM and hTIM derived from the last 4 ns of the simulations on their corresponding X-ray structures shows that both enzymes exhibit little conformational changes relative to the crystallographic structures (RMSD of 1.5 Å and 1.2 Å for TcTIM and hTIM, respectively). However, loop 6 of TcTIM that is in the closed conformation in the X-ray structure changes to the open form during the simulation (Fig. 4A). In hTIM in which both monomers have loop 6 in the open conformation in the x-ray structure this loop remains in the open state along the simulation time (Fig. 4B). The opening of loop 6 in TcTIM is an interesting result since it is the preferred conformation in apo-TIM. Therefore, the average structure obtained after MD simulations would be more representative of the predominant enzyme conformation

available in solution for accommodating the substrate or inhibitors. In order to get insight into the preferred binding modes of inhibitors in the absence of the crystal environment the average structure obtained from MD was used in subsequent docking calculations for both enzymes.

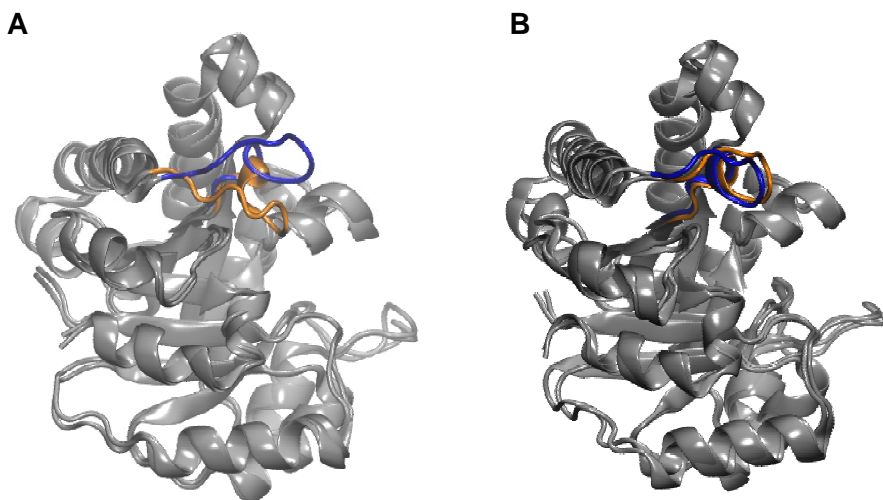


Fig. 4. Loop 6 conformations in the crystal (orange) and in the average structures (blue) of TcTIM and hTIM.
(A) Monomer A of TcTIM. (B) Monomer A of hTIM.

3.2. Insight into the binding modes and inhibition mechanisms by molecular docking and MD simulations

In order to predict the binding mode of compounds 1-3 into TcTIM molecular docking and MD simulations were performed. The aim of MD simulations was to obtain ligand-protein structures closer to physiological conditions and to examine conformational and dynamical variation of the enzyme upon ligand binding. Since the reliability of a docking result depends on the similarity of its final docked conformations the fifty docking conformations were clustered using a RMSD tolerance of 2.0 Å. For compound 1 a single cluster was obtained locating the molecule into monomer A active site. This result is consistent with the aforementioned differences between monomers. For compounds 2 and 3 all clusters showed the same binding site with alternative

conformations. In these cases the lowest energy conformation of the most populated cluster was taken as input for MD simulations. Fig. 5A–C shows that after MD simulations position and/or orientation of inhibitors in the predicted binding site were changed and this observation highlights the importance of performing simulations after docking to obtain more precise ligand-enzyme models. The RMSDs of all compounds show a drastic increase relative to the docked conformation with values ranging from 3.2 Å to 4.4 Å (Fig. 5D). These RMSD values indicate that conformation of the ligands is notoriously affected when protein flexibility is considered. After these rapid conformational changes ligands remain stable along the production phase of the simulation validating the binding site predicted by docking. Concerning the stability of enzyme-inhibitor complexes C α RMSD curves indicate that after 3.0 ns the systems reach equilibrium (see Fig. S1 in Supplementary Material). Therefore, the average structures of TcTIM-inhibitor complexes derived from the last 2 ns of the trajectories were used to analyze protein-inhibitor interactions.

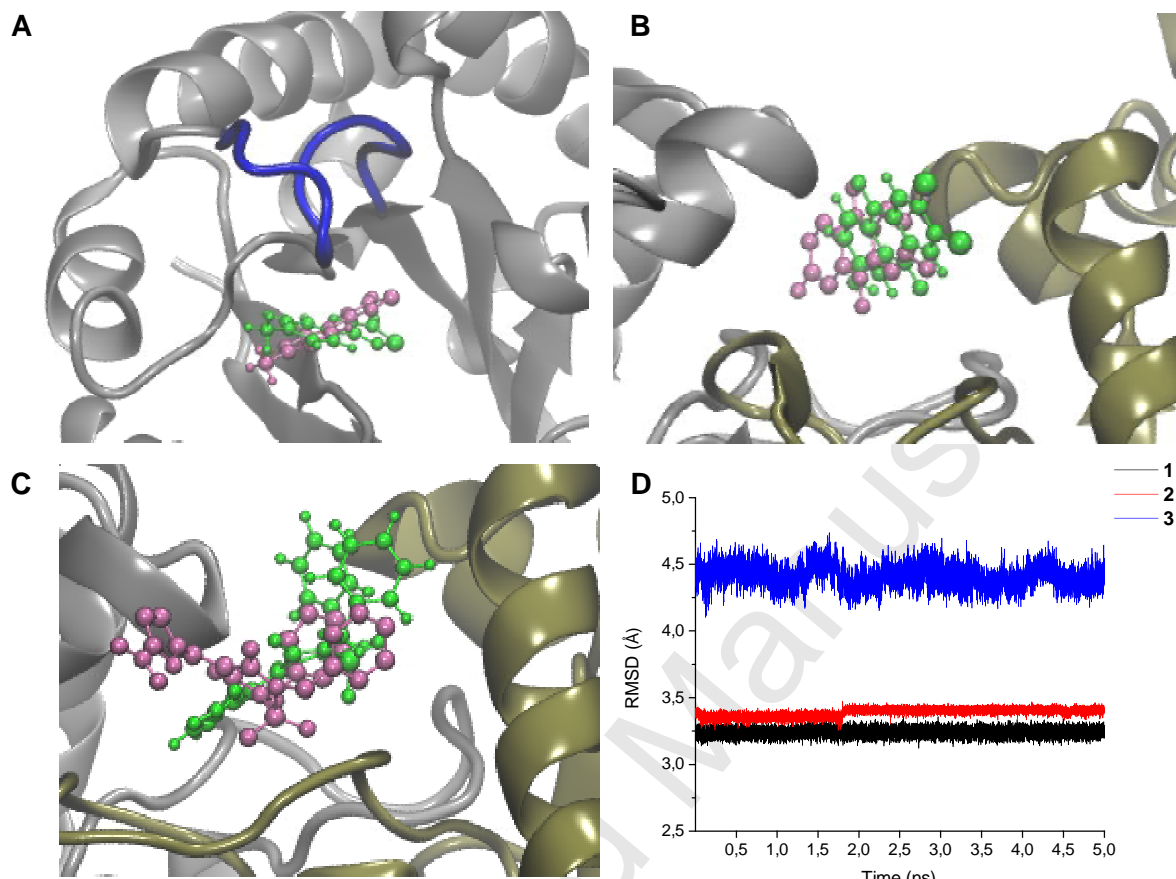


Fig. 5. Reorientation and stabilization of inhibitors after MD simulations. Docking conformations are depicted in purple and average conformations after MD simulations are shown in green. (A) Compound 1 in the active site. Loop 6 is depicted in blue. (B) Compound 2 at the dimer interface. Monomers A and B are depicted in gray and tan, respectively. (C) Compound 3 at the dimer interface. Monomers A and B are depicted in gray and tan, respectively. (D) RMSD of ligands' atoms from the starting docking structure along the production phase of the simulation.

Compound 1 binds into TcTIM active site close to the catalytic residues His95 and Lys12 (Fig. 6A). The tolyl-substituent of 1 is adjusted to fit the hydrophobic cavity containing residues Ile171, Gly211, Val213 and Gly233. The 1,2,4-thiadiazole ring makes π - π interactions with His95 and the heterocyclic NH group of the ligand forms a hydrogen bond with the backbone oxygen atom of Gly210.

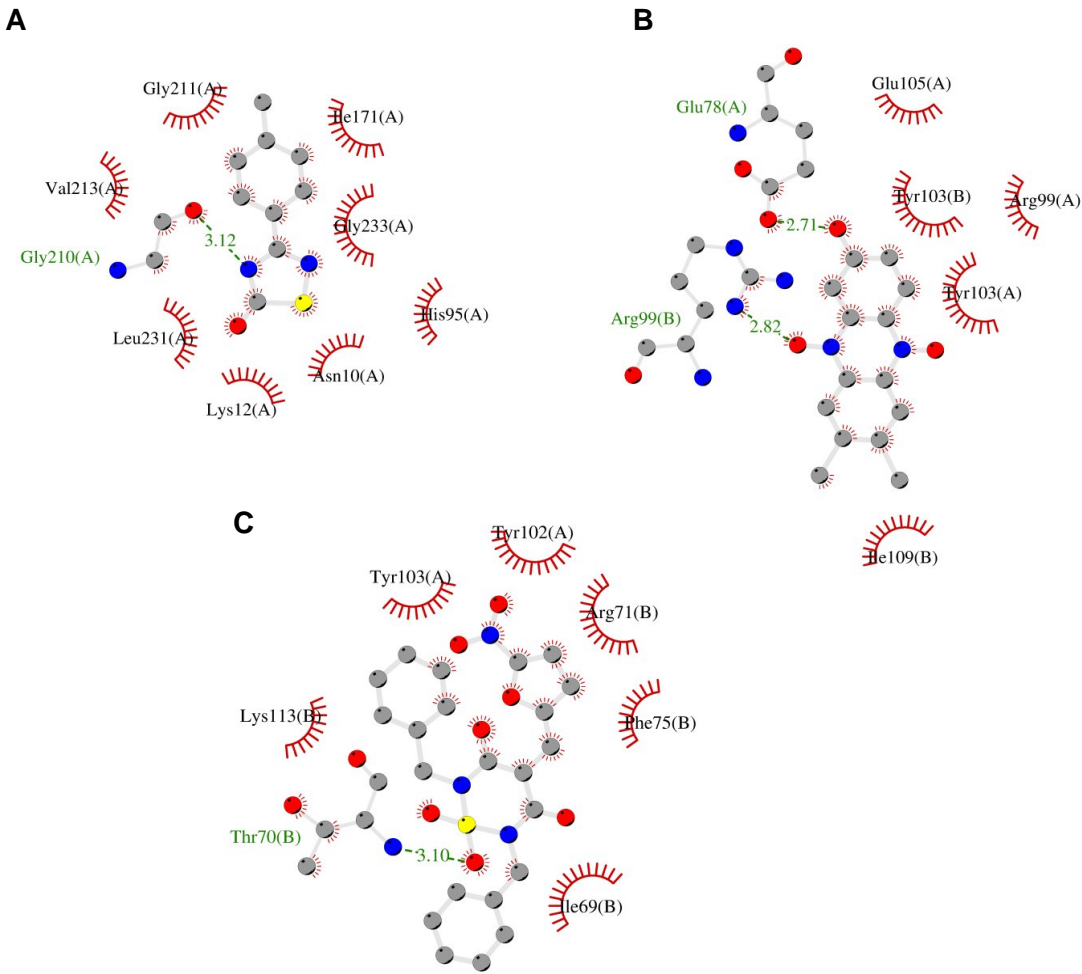
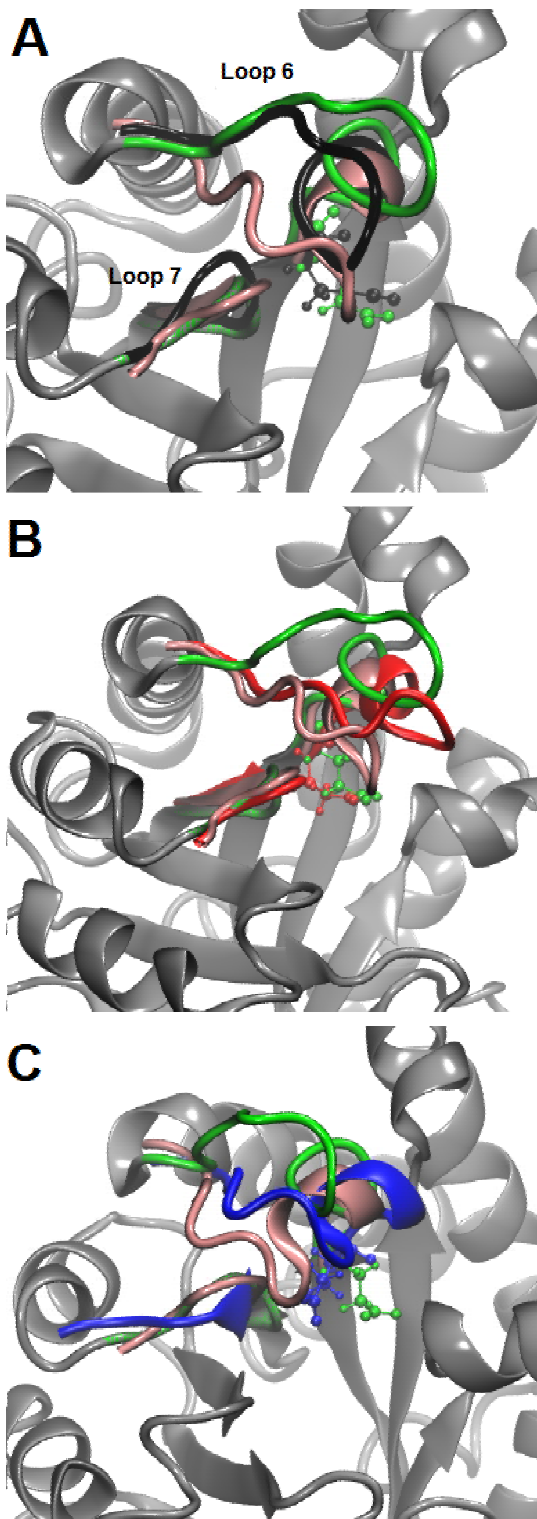


Fig. 6. Schematic diagram of TcTIM-ligand interactions generated by LigPlot+ [48]. (A) Compound 1 at the active site of monomer A. (B) Compound 2 at the dimer interface. (C) Compound 3 at the dimer interface. Hydrogen bonds are depicted as green dashed lines. Hydrophobic contacts with the ligand are presented by red semi-circles with radiating spokes.

Although 1 binds to the active site, there is experimental evidence indicating that it acts as a non-competitive inhibitor [30]. Our theoretical results are able to explain this observation showing that inhibitor binding causes a conformational change in the active site region. Figure 7A illustrates that upon ligand binding loop 6 and loop 7 adopt a different conformation compared with the native

enzyme that could alter the coordinated motion of both loops that is essential for proper enzyme dynamics and catalytic activity [49]. Moreover, the catalytic residue Glu165 remains in its "swung-out" conformation, incompatible with proper positioning and retention of the substrate for catalysis in the active site. This type of unusual non-competitive inhibition has been observed in molecules that form very stable enzyme-inhibitor complexes [50]. In our case, previous NMR experiments have confirmed the strong binding character of compound 1 into TcTIM [30].

Compounds 2 and 3 bind at the dimer interface and induce conformational changes (see below) that propagate to the active site. Compound 2 is stabilized by hydrophobic, electrostatic and hydrogen bond interactions with residues of both monomers (Fig. 6B). The phenazine ring of the inhibitor establishes π - π stacking interactions with the phenol ring of Tyr103 in monomers A and B. Moreover, one of the phenyl moieties of the phenazine forms π -cation interactions with the positively charged Arg99 residue of monomer A while the other phenyl group establishes hydrophobic interactions with Ile109 in monomer B. The oxygen atom of one of the N-oxide groups and the OH moiety of the ligand are hydrogen bonded to the NH₂ of Arg99 (monomer B) and the Oε1 atom of Glu78 (monomer A), respectively.



Binding of compound 2 to the interface causes an allosteric perturbation of loop 6 conformation which, like in TcTIM-1 complex, is maintained in the open state unsuitable for catalysis as can be seen by the position of Glu165 residue (Fig. 7B). The open state of loop 6 upon compound 2 binding is consistent with experimental data showing that compounds 1 and 2 have additive effects [19] and therefore the presence of the latter does not prevent the binding of 1 into the active site.

Compound 3 is stabilized at the dimer interface by hydrophobic interactions between its aromatic moieties and residues Tyr102, Tyr103 of monomer A and Ile69, Arg71, Phe75 and Lys113 of monomer B (Fig. 6C). In addition, the sulfonamide moiety of the ligand establishes a hydrogen bond with the backbone nitrogen of Thr70 of monomer B.

Fig. 7. Cartoon rendering of loop 6 and loop 7 conformations in TcTIM. (A) Comparison of loop 6 and loop 7 conformations in TcTIM-1 complex (black) with

apo-TcTIM in the open form (green) and TcTIM-substrate in the closed form (pink, PDB ID 1NEY). Glu165 is depicted in ball and sticks. (B) TcTIM-2 complex is depicted in red with apo-TcTIM, TcTIM-substrate complex

and Glu165 rendered in the same scheme used in (A). (C) TcTIM-3 complex is depicted in blue with apo-TcTIM, TcTIM-substrate complex and Glu165 rendered in the same scheme used in (A) and (B).

Effects caused by compound 3 on the active site conformation are shown in Fig. 7C. Binding of compound 3 seems to stabilize the Glu165 residue in the catalytically favorable “swung-in” conformation with the subsequent closing of loop 6. In this state, substrate access to the active site would be blocked. Interestingly, the theoretically predicted closure of loop 6 is consistent with experimental data indicating that compounds 3 and 1 have competitive effects, with 1 requiring higher doses to inhibit the enzyme when incubated in the presence of 3 [19]. The movement of Glu165 side chain to the “swing-in” conformation as a consequence of inhibitor binding to the dimer interface has been reported for a benzothiazole derivative [51]. It is interesting to mention that this inhibitor establishes interactions with Phe75 and Arg71 residues of chain A and Tyr102 of chain B and the change in position of Glu165 occurs only in the active site of chain A. However, for compound 3 that interacts with several residues of both chains Glu165 displacement occurs in both active sites.

According to our theoretical results, the three inhibitors cause alterations into the active site conformation that could lead to a loss of enzyme activity upon ligand binding. However, since these three compounds have different inhibitory potency further analyzes were performed to determine how inhibitor binding affects the global structure and dynamics of TcTIM and to advance in the understanding of the mechanism by which each compound exert its inhibitory function. Fig. 8 reports the root mean square fluctuation (RMSF) of backbone C α atoms for free and bound TcTIM. Firstly, for apo-TcTIM the comparison of calculated RMSF with experimental

crystallographic temperature factors (B-factor, Fig. 8A) shows a good correlation, confirming that our MD simulations are able to adequately recreate the behavior of the real protein.

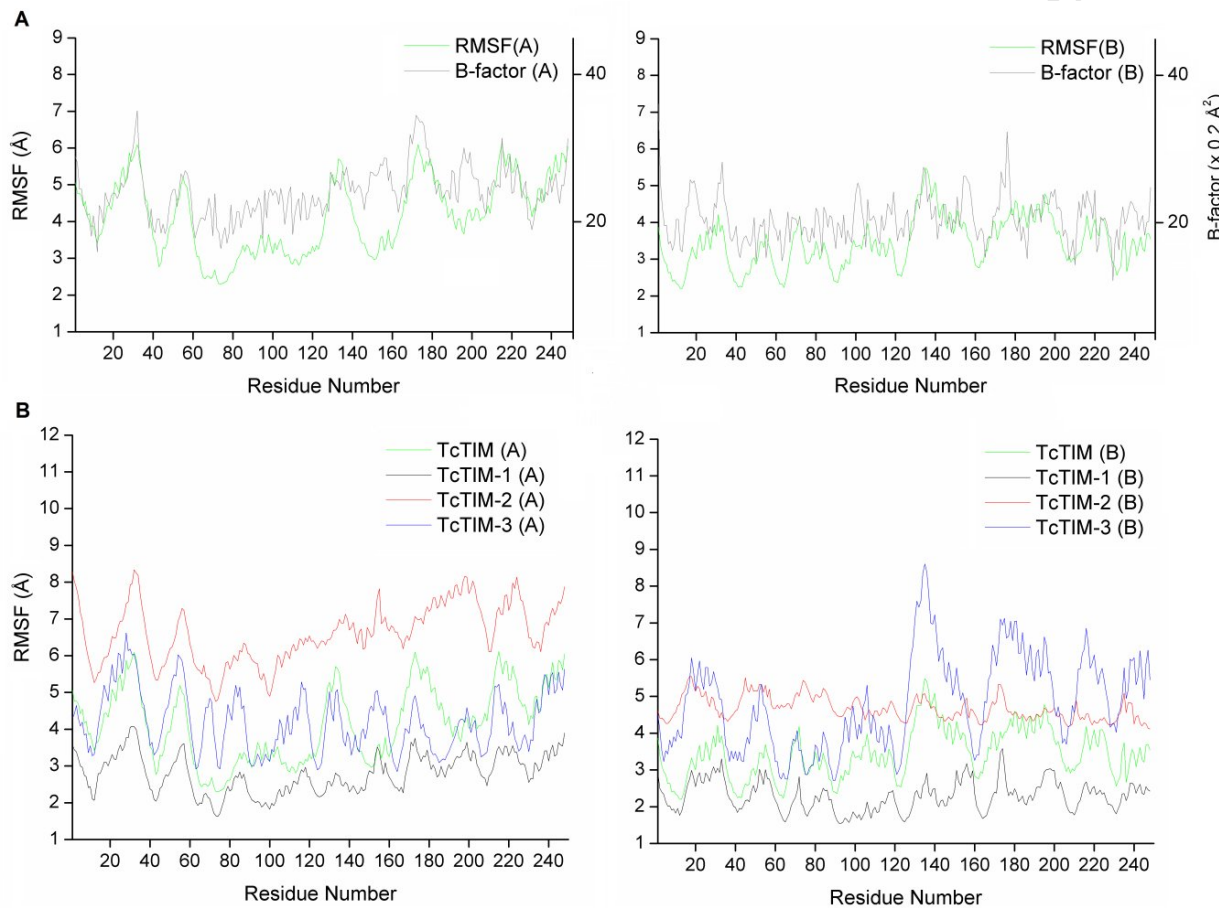


Fig. 8. RMSF of backbone $\text{C}\alpha$ atoms along MD simulations. (A) Comparison of apo-TcTIM RMSF values (green) with crystallographic B-values (gray, PDB ID: 1TCD). (B) Comparison of RMSF values for free and bound TcTIM. Apo-TcTIM is shown in green. TcTIM-1, TcTIM-2 and TcTIM-3 complexes are shown in black, red and blue, respectively.

Comparing the RMSF profiles of apo- and inhibitor-bound TcTIM (Fig. 8B) it can be seen that all inhibitors alter enzyme flexibility. Interestingly, the most potent inhibitor (compound 1) causes a significant decrease in enzyme mobility in both monomers. This loss of conformational flexibility upon compound 1 binding suggests that this inhibitor could be preventing essential motions of the

enzyme required for optimal activity. The reduction in enzyme mobility is in accordance with the formation of a very stable enzyme-inhibitor complex as determined experimentally and supports the observation that compound 1 could lock the active site into an inactive conformation (see above). Compound 2, the less potent inhibitor against TcTIM (Fig. 1), exhibit high RMSF values for both monomers. This remarkable increase in enzyme flexibility together with the binding of 2 at the dimer interface could lead to a weakening of monomer-monomer interactions and the subsequent drop in enzyme activity by disruption of the dimer integrity. In fact, changes in solvent accessible surface area (SASA) for residues involved in joining together the two monomers (see Fig. S2 in Supplementary Material) agree well with compound 2 inhibiting TcTIM activity by dimer disruption. However, the access of the substrate to the active site would not be affected since loop 6 would be still able to freely fluctuate between open and close conformations and this is in agreement with the experimental observation that compounds 1 and 2 have additive effects. Compound 3 with an IC₅₀ against TcTIM between 1 and 2 shows a distinct fashion of RMSF change depending on the sequence (Fig. 8B). In some regions (residues 1 to 140) RMSF profile is not affected by the inhibitor while loop 6/loop 7 regions of monomer A (residues 166-176/209-213) show a decrease in flexibility. This decrease in flexibility is consistent with experimental data showing that compounds 1 and 3 have competitive effects since loop 6 would be stabilized in the closed conformation blocking compound 1 or substrate access. Residues of monomer B experiment an increase in flexibility due to ligand binding and this could lead to an alteration of inter-monomer contacts as indicated by changes in the SASA of many interfacial residues (Fig. S2). The behavior of the enzyme after inhibitors 2 and 3 binding agree well with these compounds acting as dimer-disrupting inhibitors of TcTIM as was previously reported [19]. The low flexibility of active loop 6 in TcTIM-3 complex may explain the better inhibitory power of this compound relative to compound 2. It is worth noticing that since compounds 2 and 3 are mild inhibitors of

TcTIM, residues that constitute their binding sites can be considered as “hot spots” [52] that should be taken into account in the design of new dimer-disrupting molecules with a better inhibitory profile.

3.3. Insights into compound 1 selectivity against TcTIM

Inhibitory molecules that bind the dimer interface like compounds 2 and 3 are expected to have high selectivity against TcTIM due to the low percentage of identity (36%) between trypanosomal and human enzymes for residues which make up the binding site of these inhibitors. However, since compound 1 binds into the active site a high selectivity degree against TcTIM would not be expected. In order to understand the selectivity displayed by this compound, docking and MD simulations were performed to predict the binding mode of 1 into hTIM.

As shown in Fig. 9 compound 1 binds to monomer B of hTIM into a solvent exposed cleft behind loop 7 making hydrogen bond interactions with Ser211. Although loop 7 changes its conformation to accommodate the compound, loop 6 remains in the open conformation with the catalytic Glu165 in the “swung-out” conformation characteristic of the apo-enzyme. At a first glance, the binding pose of compound 1 could be competing with substrate binding since the backbone NH group of Ser211 provides hydrogen bond to the phosphate moiety of the substrate, helping to stabilize it. Furthermore, Ala176 and Tyr208 lining the binding site of 1 have a crucial role in loop 6 closing to form the binding pocket for the substrate’s phosphate dianion [53]. However, the poor inhibitory activity of 1 against hTIM could be explained looking at the high flexibility of the human enzyme, which is maintained or even increased in some regions after compound 1 binding (Fig. 10A). This remarkable mobility might promote an easy and rapid expulsion of the ligand from it

solvent accessible binding site. The fact that is actually harder to hit a moving target has been largely discussed; see [54] and references therein.

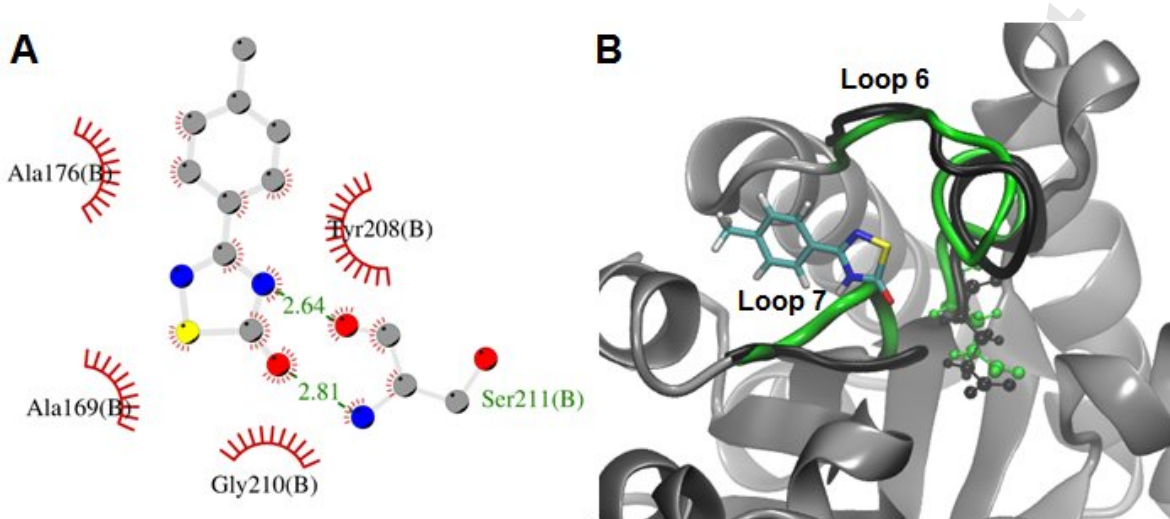


Fig. 9. Compound 1-bound hTIM. (A) Schematic diagram of hTIM-1 interactions. (B) Cartoon rendering of compound 1 binding site showing loop 6 and loop 7 conformations in apo-hTIM (green) and hTIM-1 complex (black). Compound 1 is depicted in sticks and the catalytic Glu165 in ball and sticks.

Unlike to what is observed in TcTIM, the RMSD profile as indicator of the conformational stability of the enzyme shows little change upon compound 1 binding (Fig. 10B) and this is consistent with the formation of a weak ligand-enzyme complex where the ligand is unable to affect the global structure of the enzyme. Regarding this observation, it is worth noting that interactions mediated by Glu104 at the dimer interface, whose disruption in mutants has been associated with hTIM deficiency [55], are not significantly affected upon compound 1 binding (see Fig. S3 in Supplementary Material).

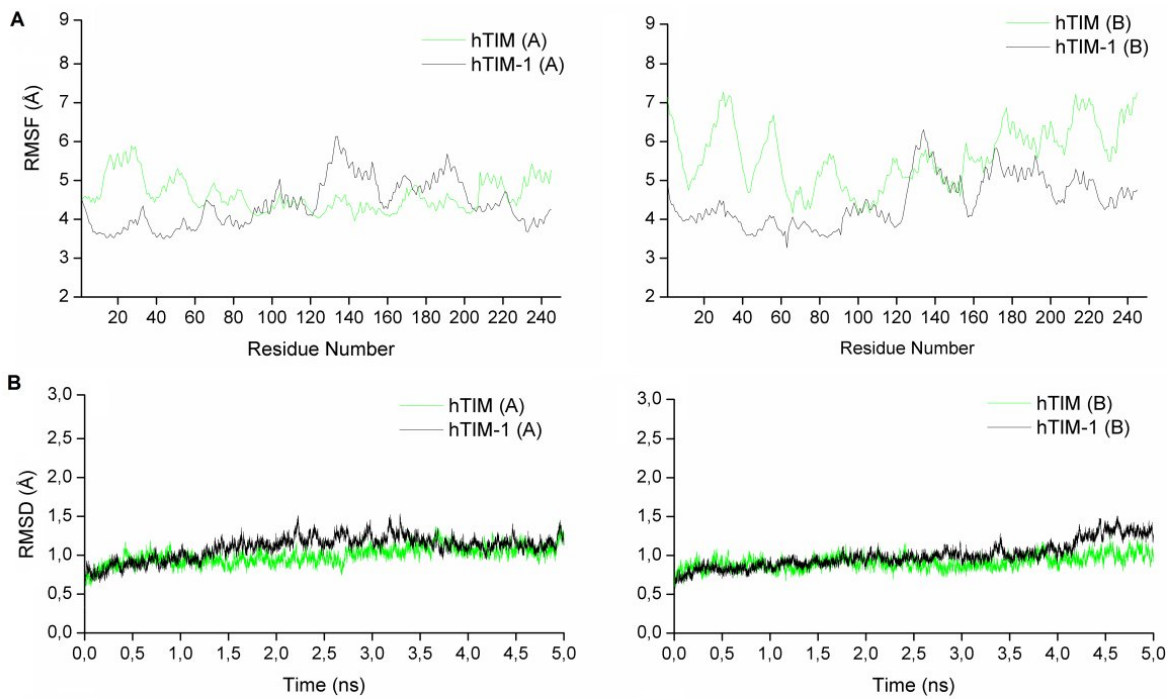


Fig. 10. Comparative analysis of the MD trajectories for apo-hTIM and hTIM-1 complex. (A) RMSF of the C α atoms of monomer A (left) and B (right) for the two systems. (B) C α RMSD of monomer A (left) and B (right) for the two systems.

4. Conclusions

In this study we have predicted the binding mode and mechanism of action of 1,2,4-thiadiazole (1), phenazine 5,10-dioxide (2) and 1,2,6-thiadiazine (3) derivatives into TcTIM. The binding mode of 1 to hTIM was also determined. Compounds 2 and 3 bind at the dimer interface of TcTIM and exert their action through the perturbation of the dimer integrity. On the other hand, compound 1 binds into the active site causing a significant decrease in enzyme mobility in both monomers. This loss of conformational flexibility upon compound 1 binding suggests that this inhibitor could be acting by preventing essential motions of the enzyme required for optimal activity. Interestingly, the binding of compound 3 at the dimer interface changes loop 6 conformation, stabilizing it in the

closed state and therefore blocking compound 1 access. This explains the experimentally observed competitive behavior between both compounds. The low inhibitory activity of 1 against hTIM was also investigated and seems to be related with the high flexibility of this enzyme that would hinder the formation of a stable ligand-enzyme complex. Our theoretical results are consistent with previous experimental data and have provided us with useful information for future prospects on rational drug design.

Acknowledgment

The Program for Development of the Basic Sciences (PEDECIBA-Química, UDELAR-UNDP-Uruguayan government) is gratefully acknowledged for financial support. MG, HC, GA and AM are members of the National System of Researchers (SNI-ANII, Uruguay) whose support is also gratefully acknowledged. We thank ANII for the scholarship to LM.

References

- [1] F.X. Lescure, G. Le Loup, H. Freilij, M. Developoux, L. Paris, L. Brutus, G. Pialoux, Chagas disease: changes in knowledge and management, Lancet Infect. Dis. 10 (2010) 556-570.
- [2] <http://www.treatchagas.org/>, accessed May 2013.
- [3] B.Y. Lee, K.M. Bacon, M.E. Botazzi, P.J. Hotez, Global economic burden of Chagas disease: a computational simulation model, Lancet Infect. Dis. 13 (2013) 342-348.
- [4] P.M.M. Guedes, G.K. Silva, F.R.S. Gutierrez, J.S. Silva, Current status of Chagas disease chemotherapy, Expert Rev. Anti Infect. Ther. 9 (2011) 609-620.

- [5] J.C. Vázquez-Chagoyán, S. Gupta, N.J. Garg, Vaccine development against *Trypanosoma cruzi* and Chagas disease, *Adv. Parasitol.* 75 (2011) 121-146.
- [6] S. Nwaka, A. Hudson, Innovative lead discovery strategies for tropical diseases, *Nat. Rev. Drug Discov.* 5(2006) 941-955.
- [7] M. González, H. Cerecetto, Novel compounds to combat trypanosomatid infections: a medicinal chemical perspective, *Expert Opin. Ther. Pat.* 21 (2011) 699-715.
- [8] M. de Nazaré, C. Soeiro, S. Lisboa de Castro, Screening of potential anti-*Trypanosoma cruzi* candidates: in vitro and in vivo studies, *Open Med. Chem. J.* 5 (2011) 21-30.
- [9] C.L. Verlinde, V. Hannaert, C. Blonski, M. Willson, J.J. Périé, L.A. Fothergill-Gilmore, F.R. Opperdoes, M.H. Gelb, W.G. Hol, P.A. Michels, Glycolysis as a target for the design of new anti-trypanosome drugs, *Drug Resist. Updat.* 4 (2001) 50-65.
- [10] S. Enriquez-Flores, A. Rodríguez-Romero, G. Hernández-Alcantara, I. De la Mora-De la Mora, P. Gutiérrez-Castellón, K. Carvajal, G. López-Velázquez, H. Reyes-Vivas, Species-specific inhibition of *Giardia lamblia* triosephosphate isomerase by localized perturbation of the homodimer, *Mol Biochem. Parasitol.* 157 (2008) 179–186.
- [11] A. Rodríguez-Romero, A. Herrández-Santoyo, L. del Pozo Yauner, A. Kornhauser, D.A. Fernández-Velasco, Structure and inactivation of triosephosphate isomerase from *Entamoeba histolytica*, *J. Mol. Biol.* 322 (2002) 669-675.
- [12] E. Maldonado, M. Soriano-García, A. Moreno, N. Cabrera, G. Garza-Ramos, Differences in intersubunit contacts in thriosephosphate isomerase from two closely related pathogenic parasites, *J. Mol. Biol.* 283 (1998) 193-203.
- [13] S.S. Velanker, S.S. Ray, R.S. Gokhale, S. Suma, H. Balaram, P. Balaram, M.R.N. Murthy, Triosephosphate isomerase from *Plasmodium falciparum*: the crystal structure provides insights into antimalarial drug design, *Structure* 5 (1997) 751-761.

- [14] J.R. Knowles, Enzyme-catalysis: not different, just better, *Nature* 350 (1991) 121-124.
- [15] G. Álvarez, B. Aguirre-López, J. Varela, M. Cabrera, A. Merlino, G.V. López, M.L. Lavaggi, W. Porcal, R. Di Maio, M. González, H. Cerecetto, N. Cabrera, R. Pérez-Montfort, M. Tuena de Gómez-Puyou, A. Gómez-Puyou, Massive screening yields novel and selective Trypanosoma cruzi triosephosphate isomerase dimer-interface-irreversible inhibitors with anti-trypanosomal activity, *Eur. J. Med. Chem.* 45 (2010) 5767-5772.
- [16] V. Olivares-Illana, A. Rodríguez-Romero, I. Becker, M. Berzunza, J. García, R. Pérez-Montfort, N. Cabrera, F. López-Calahorra, M. Tuena de Gómez-Puyou, A. Gómez-Puyou . Perturbation of the dimer interface of triosephosphate isomerase and its effect on Trypanosoma cruzi, *PLoS Negl. Trop. Dis.* 1 (2007) e01.
- [17] V. Olivares-Illana, R. Pérez-Montfort, F. López-Calahorra, M. Costas, A. Rodríguez-Romero, M. Tuena de Gómez-Puyou, A. Gómez-Puyou, Structural differences in triosephosphate isomerase from different species and discovery of a multitypanosomatid inhibitor, *Biochemistry* 45 (2006) 2556-2560.
- [18] A. Tellez-Valencia, S. Ávila-Ríos, R. Pérez-Montfort, A. Rodríguez-Romero, M. Tuena de Gómez-Puyou, F. López-Calahorra, A. Gómez-Puyou, Highly specific inactivation of triosephosphate isomerase from Trypanosoma cruzi, *Biochem. Biophys. Res. Commun.* 295 (2002) 958-963.
- [19] G. Álvarez, J. Martínez, B. Aguirre-López, N. Cabrera, L. Pérez-Díaz, M. Tuena de Gómez-Puyou, A. Gómez-Puyou, R. Pérez-Montfort, B. Garat, A. Merlino, M. González, H. Cerecetto, New chemotypes as Trypanosoma cruzi triosephosphate isomerase inhibitors. A deeper insight into the mechanism of inhibition, *J. Enz. Inhib. Med. Chem.* 29 (2014) 198-204.
- [20] A. Romo-Mancillas, A. Tellez-Valencia, L. Yepez-Mulia, F. Hernández-Luis, A. Hernández-Campos, R. Castillo, The design and inhibitory profile of new benzimidazole derivatives against

triosephosphate isomerase from *Trypanosoma cruzi*: A problem of residue motility, *J. Mol. Graph. Model.* 30 (2011) 90-99

- [21] R. Chavez-Calvillo, M. Costas, J. Hernández-Trujillo, Theoretical analysis of intermolecular interactions of selected residues of triosephosphate isomerase from *Trypanosoma cruzi* with its inhibitor 3-(2-benzothiazolylthio)-1-propanesulfonic acid, *Phys. Chem. Chem. Phys.* 12 (2010) 2067–2074.
- [22] L.M. Espinoza-Fonseca, J.G. Trujillo-Ferrara, Toward a rational design of selective multitypanosomatid inhibitors: a computational docking study, *Bioorg. Med. Chem. Lett.* 16 (2006) 6288–6292.
- [23] L.M. Espinoza-Fonseca, J.G. Trujillo-Ferrara, Structural considerations for the rational design of selective anti-trypanosomal agents: the role of the aromatic clusters at the interface of triosephosphate isomerase dimer, *Biochem. Biophys. Res. Commun.* 328 (2005) 922–928.
- [24] L.M. Espinoza-Fonseca, J.G. Trujillo-Ferrara, Exploring the possible binding sites at the interface of triosephosphate isomerase dimer as a potential target for anti-trypanosomal drug design, *Bioorg. Med. Chem. Lett.* 14 (2004) 3151-3154.
- [25] S-Y. Huang, X. Zou, Advances and challenges in protein-ligand docking, *Int. J. Mol. Sci.* 11 (2010) 3016-3034.
- [26] J.G. Kempf, J-Y. Jung, C. Ragain, N.S. Sampson, J.P. Loria, Dynamic requirements for a functional protein hinge, *J. Mol. Biol.* 368 (2007) 131-149.
- [27] H. Alonso, A.A. Bliznyuk, J.E. Gready, Combining docking and molecular dynamics simulations in drug design, *Med. Chem. Rev.* 26 (2006) 531-568.
- [28] M.A. Lill, Efficient incorporation of protein flexibility and dynamics into molecular docking simulations, *Biochemistry* 50 (2011) 6157-6169.

- [29] Z. Wang, B. Ling, R. Zhang, Y. Liu, Docking and molecular dynamics study on the inhibitory activity of coumarins on aldose reductase, *J. Phys. Chem. B* 32 (2008) 10033-10040.
- [30] G. Álvarez, B. Aguirre-López, N. Cabrera, E.B. Marins, L. Tinoco, C.I. Batthyany, M. Tuena de Gómez- Puyou, A. Gómez-Puyou, R. Pérez-Montfort, H. Cerecetto , M. González, 1,2,4-thiadiazol-5(4H)-ones: a new class of selective inhibitors of Trypanosoma cruzi triosephosphate isomerase. Study of the mechanism of inhibition, *J. Enz. Inhib. Med. Chem.* 28 (2013) 981-989.
- [31] D.A. Case, T.A. Darden, T.E. Cheatham, III, C.L. Simmerling, J. Wang, R.E. Duke, R. Luo, R.C. Walker, W. Zhang, K.M. Merz, B. Roberts, S. Hayik, A. Roitberg, G. Seabra, J. Swails, A.W. Goetz, I. Kolossvai, K.F. Wong, F. Paesani, J. Vanicek, R.M. Wolf, J. Liu, X. Wu, S.R. Brozell, T. Steinbrecher, H. Gohlke, Q. Cai, X. Ye, J. Wang, M.-J. Hsieh, G. Cui, D.R. Roe, D.H. Mathews, M.G. Seetin, R. Salomon-Ferrer, C. Sagui, V. Babin, T. Luchko, S. Gusarov, A. Kovalenko, P.A. Kollman (2012), AMBER 12, University of California, San Francisco.
- [32] Y. Duan, C. Wu, S. Chowdhury, M. C. Lee, G. Xiong, W. Zhang, R. Yang, P. Cieplak, R. Luo, T. Lee, J. Caldwell, J. Wang, P. Kollman, A point-charge force field for molecular mechanics simulations of proteins based on condensed-phase quantum mechanical calculations, *J. Comput. Chem.* 24 (2003) 1999-2012.
- [33] W.L. Jorgensen, J. Chandrasekhar, J.D. Madura, R.W. Impey, M. L. Klein, Comparison of simple potential functions for simulating liquid water, *J. Chem. Phys.* 79 (1983) 926-935.
- [34] U. Essmann, L. Perera, M.L. Berkowitz, T. Darden, H. Lee, L.G. Pedersen, A smooth particle mesh Ewald method, *J. Chem. Phys.* 103 (1995) 8577-8593.
- [35] H.J.C. Berendsen, J.P.M. Postma, W.F. van Gunsteren, A. DiNola, J.R. Haak, Molecular dynamics with coupling to an external bath, *J. Chem. Phys.* 81 (1984) 3584-3690.
- [36] R.W. Pastor, B.R. Brooks, A. Szabo, An analysis of the accuracy of Langevin and molecular dynamics algorithms, *Mol. Phys.* 65 (1988) 1409-1419.

- [37] J.P. Ryckaert, G. Ciccotti, H.J.C. Berendsen, Numerical-integration of cartesian equations of motion of a system with constraints -molecular-dynamics of N-alkanes, *J. Comput. Phys.* 23 (1977) 327-341.
- [38] A.D. Becke, Density-functional thermochemistry. III. The role of exact exchange, *J. Chem. Phys.* 98 (1993) 5648-5652.
- [39] R. Ditchfield, W.J. Hehre, J.A. Pople, Self-consistent molecular orbital methods. 9. Extended Gaussian-type basis for molecular-orbital studies of organic molecules, *J. Chem. Phys.* 54 (1971) 724-728.
- [40] M.T. Cances, B. Mennucci, J. Tomasi, A new integral equation formalism for the polarizable continuum model: theoretical background and applications to isotropic and anisotropic dielectrics, *J. Chem. Phys.* 107 (1997) 3032-3041.
- [41] M.J. Frisch, G.W. Trucks, H.B. Schlegel, G.E. Scuseria, M.A. Robb, J.R. Cheeseman, G. Scalmani, V. Barone, B. Mennucci, G.A. Petersson, H. Nakatsuji, M. Caricato, X. Li, H. P. Hratchian, A.F. Izmaylov, J. Bloino, G. Zheng, J.L. Sonnenberg, M. Hada, M. Ehara, K. Toyota, R. Fukuda, J. Hasegawa, M. Ishida, T. Nakajima, Y. Honda, O. Kitao, H. Nakai, T. Vreven, J.A. Montgomery, Jr., J.E. Peralta, F. Ogliaro, M. Bearpark, J.J. Heyd, E. Brothers, K.N. Kudin, V.N. Staroverov, R. Kobayashi, J. Normand, K. Raghavachari, A. Rendell, J.C. Burant, S.S. Iyengar, J. Tomasi, M. Cossi, N. Rega, J.M. Millam, M. Klene, J.E. Knox, J.B. Cross, V. Bakken, C. Adamo, J. Jaramillo, R. Gomperts, R.E. Stratmann, O. Yazyev, A.J. Austin, R. Cammi, C. Pomelli, J.W. Ochterski, R.L. Martin, K. Morokuma, V.G. Zakrzewski, G.A. Voth, P. Salvador, J.J. Dannenberg, S. Dapprich, A.D. Daniels, Ö. Farkas, J.B. Foresman, J.V. Ortiz, J. Cioslowski, D.J. Fox. Gaussian 09, Revision A.02, Gaussian Inc., Wallingford CT, 2009.

- [42] G.M. Morris, R. Huey, W. Lindstrom, M.F. Sanner, R.K. Belew, D.S. Goodsell, A.J. Olson, AutoDock4 and AutoDockTools4: Automated docking with selective receptor flexibility, *J. Comput. Chem.* 30 (2009) 2785-2791.
- [43] J.M. Wang, R.M. Wolf, J.W. Caldwell, P.A. Kollman, D.A. Case, Development and testing of a general amber force field, *J. Comput. Chem.* 25 (2004) 1157-1174.
- [44] Z. Kurkcuoglu, A. Bakan, D. Kocaman, I. Bahar, P. Doruker, Coupling between catalytic loop motions and enzyme global dynamics, *PLOS Comput. Biol.* 8 (2012) e1002705.
- [45] S. Rozovsky, A.E. McDermott, The time scale of the catalytic loop motion in Triosephosphate Isomerase, *J. Mol. Biol.* 310 (2001) 259-270.
- [46] J.P. Loria, R.B. Berlow, E.D. Watt, Characterization of enzyme motions by solution NMR relaxation dispersion, *Acc. Chem. Res.* 41 (2008) 214-221.
- [47] R.K. Wierenga, M.E.M. Noble, G. Vriend, S. Nauche, Refined 1.83 Å structure of trypanosomal Triosephosphate Isomerase crystallized in the presence of 2.4 M ammonium sulphate, *J. Mol. Biol.* 220 (1991) 995-1015.
- [48] A.C. Wallace, R.A. Laskowski, J.M. Thornton, LIGPLOT: A program to generate schematic diagrams of protein-ligand interactions, *Prot. Eng.* 8 (1995) 127-134.
- [49] Y. Wang, R.B. Berlow, J.P. Loria, Role of loop-loop interactions in coordinating motions and enzymatic function of triosephosphate isomerase, *Biochemistry* 48 (2009) 4548-4556.
- [50] Y. Blat, Non-competitive inhibition by active site binders, *Chem. Biol. Drug Des.* 75 (2010) 535-540.
- [51] A. Téllez-Valencia, V. Olivares-Illana, A. Hernández-Santoyo, R. Pérez-Montfort, M. Costas, A. Rodríguez-Romero, F. López Calahorra, M. Tuena de Gómez-Puyou, A. Gómez-Puyou, Inactivation of triosephosphate isomerase from *Trypanosoma cruzi* by an agent that perturbs its dimer interface, *J. Mol. Biol.* 341 (2004) 1355-1365.

- [52] D. Kozakov, D.R. Hall, G.Y. Chuang, R. Cencic, R. Brenke, L.E. Grove, D. Beglov, J. Pelletier, A. Whitty, S. Vajda, Structural conservation of druggable hot spots in protein–protein interfaces PNAS, 108 (2011) 13528-13533.
- [53] R. Wierenga, E. Kapetaniou, R. Venkatesan, Triosephosphate isomerase: a highly evolved biocatalyst, Cell. Mol. Life Sci. 67 (2010) 3961-3982.
- [54] A. Ivetac, J.A. McCammon, Molecular recognition in the case of flexible targets, Curr. Pharm. Des. 17 (2011) 1663-1671.
- [55] C. Rodríguez-Almazán, R. Arreola, D. Rodríguez-Larrea, B. Aguirre-López, M. Tuena de Gómez-Puyou, R. Pérez-Montfort, M. Costas, A. Gómez-Puyou, A. Torres-Larios, Structural basis of human triosephosphate isomerase deficiency: mutation E104D is related to alterations of a conserved water network at the dimer interface, J. Biol. Chem. 283 (2008) 23254-23263.

Figure captions

Fig. 1. Chemical structures and inhibitory activity of compounds used in this study.

Fig. 2. Comparison of Ca RMSD (relative to the energy minimized starting structure) as a function of time for TcTIM (solid black line) and hTIM (dashed red line) along 5 ns MD simulations.

Fig. 3. Ca RMSF of monomers A and B for TcTIM (A) and hTIM (B). L3, L6 and L7 refer to loop 3, loop 6 and loop 7, respectively.

Fig. 4. Loop 6 conformations in the crystal (orange) and in the average structures (blue) of TcTIM and hTIM. (A) Monomer A of TcTIM. (B) Monomer A of hTIM.

Fig. 5. Reorientation and stabilization of inhibitors after MD simulations. Docking conformations are depicted in purple and average conformations after MD simulations are shown in green. (A) Compound 1 in the active site. Loop 6 is depicted in blue. (B) Compound 2 at the dimer interface.

Monomers A and B are depicted in gray and tan, respectively. (C) Compound 3 at the dimer interface. Monomers A and B are depicted in gray and tan, respectively. (D) RMSD of ligands' atoms from the starting docking structure along the production phase of the simulation.

Fig. 6. Schematic diagram of TcTIM-ligand interactions generated using LigPlot+ [48]. (A) Compound 1 at the active site of monomer A. (B) Compound 2 at the dimer interface. (C) Compound 3 at the dimer interface. Hydrogen bonds are depicted as green dashed lines. Hydrophobic contacts with the ligand are presented by red semi-circles with radiating spokes.

Fig. 7. Cartoon rendering of loop 6 and loop 7 conformations in TcTIM. (A) Comparison of loop 6 and loop 7 conformations in TcTIM-1 complex (black) with apo-TcTIM in the open form (green) and TcTIM-substrate in the closed form (pink, PDB ID 1NEY). Glu165 is depicted in ball and sticks. (B) TcTIM-2 complex is depicted in red with apo-TcTIM, TcTIM-substrate complex and Glu165 rendered in the same scheme used in (A). (C) TcTIM-3 complex is depicted in blue with apo-TcTIM, TcTIM-substrate complex and Glu165 rendered in the same scheme used in (A) and (B).

Fig. 8. RMSF of backbone C α atoms along MD simulations. (A) Comparison of apo-TcTIM RMSF values (green) with crystallographic B-values (gray, PDB ID: 1TCD). (B) Comparison of RMSF values for free and bound TcTIM. Apo-TcTIM is shown in green. TcTIM-1, TcTIM-2 and TcTIM-3 complexes are shown in black, red and blue, respectively.

Fig. 9. Compound 1-bound hTIM. (A) Schematic diagram of hTIM-1 interactions. (B) Cartoon rendering of compound 1 binding site showing loop 6 and loop 7 conformations in apo-hTIM (green) and hTIM-1 complex (black). Compound 1 is depicted in sticks and the catalytic Glu165 in ball and sticks.

Fig. 10. Comparative analysis of the MD trajectories for apo-hTIM and hTIM-1 complex. (A) RMSF of the C α atoms of monomer A (left) and B (right) for the two systems. (B) C α RMSD of monomer A (left) and B (right) for the two systems.

Supplementary Material

Fig. S1. $\text{C}\alpha$ RMSDs from the energy minimized starting structure as a function of time for, from bottom to top, free TcTIM, TcTIM-1, TcTIM-2 and TcTIM-3 complexes.

Fig. S2. Comparative analysis of the solvent accessible surface area (SASA) of interfacial residues along the simulation time for apo-TcTIM (green), TcTIM-2 (red) and TcTIM-3 (blue) complexes.

Fig. S3. Interactions mediated by Glu104 in apo-hTIM (A) and hTIM-1 complex (B).

PDB S1 The coordinates of the MD-simulated structure for apo-TcTIM

PDB S2 The coordinates of the MD-simulated structure for apo-hTIM

PDB S3 The coordinates of the MD-simulated structure for compound 1 in complex with TcTIM

PDB S4 The coordinates of the MD-simulated structure for compound 2 in complex with TcTIM

PDB S5 The coordinates of the MD-simulated structure for compound 3 in complex with TcTIM

PDB S6 The coordinates of the MD-simulated structure for compound 1 in complex with hTIM

Author Contributions

Conceived and designed the theoretical work: LM, AM. Proposed the research topic: GA, HC, MG.

Performed the theoretical calculations: LM. Analyzed the data: LM, AM. Wrote the paper: AM.

Corrected the paper and made suggestions: GA, HC, MG, LM.